Analysis of furnace slag in railway sub-ballast based on experimental tests and DEM simulations

Jia, Wenli; Markine, V. L.; Jing, Guoqing

DOI
10.1016/j.conbuildmat.2021.123114

Publication date
2021

Document Version
Final published version

Published in
Construction and Building Materials

Citation (APA)
Jia, W., Markine, V. L., & Jing, G. (2021). Analysis of furnace slag in railway sub-ballast based on experimental tests and DEM simulations. *Construction and Building Materials*, *288*, 1-8. Article 123114. https://doi.org/10.1016/j.conbuildmat.2021.123114

Construction and Building Materials 288 (2021) 123114

Contents lists available at ScienceDirect

Construction and Building Materials

journal homepage: www.elsevier.com/locate/conbuildmat

Analysis of furnace slag in railway sub-ballast based on experimental tests and DEM simulations

Wenli Jia [a], V.L. Markine [a], Guoqing Jing [b,*]

[a] Faculty of Civil Engineering and Geosciences, Delft University of Technology, Delft 2628CN, Netherlands
[b] School of Civil Engineering, Beijing Jiaotong University, Beijing 100044, China

HIGHLIGHTS

- Introducing furnace slag as railway sub-ballast.
- The breakage and abrasion properties are analysed.
- The performance of furnace slag for sub-ballast was analysed.
- A comparison between furnace slag with traditional sub-ballast.

ARTICLE INFO

Article history:
Received 14 December 2020
Received in revised form 2 March 2021
Accepted 16 March 2021

Keywords:
Furnace slag
Sub-ballast
Stiffness tests
Direct shear test
DEM

ABSTRACT

Under the high requirement of ballast materials and the frequent maintenance of high-speed and heavy-haul railway, the maintenance cost and material consumption become an important problem. Several methods are used to increase the stability and service life of railway structure, also using recycled materials in ballast bed construction can be a way for railway sustainable development. Thus, an idea of using furnace slag as the sub-ballast was put forward in this research. To qualify the performance of furnace slag, a series of tests were carried out, including single particle crushing test, direct shear test, box stiffness test, and the crushed stone which is the traditional sub-ballast material was used as a comparison. In addition, the test and numerical simulation on box stiffness were carried. Results show that furnace slag has less possible to breakage and abrasion, its shear resistance is 16.46%–19.48% higher, and 20.44%–26.04% decrease in shear dilatancy. However, the stiffness for single particle shows not much difference, the box stiffness test and simulation indicated that furnace slag has a higher capacity and better elasticity. Based on that, this research provides the feasibility of using furnace slag as the sub-ballast, and it works as an environment-friendly way in railway construction.

1. Introduction

Ballast track bed consists of two granular layers, the ballast layer and the sub-ballast layer, and it is normally constructed by crushed stone. The function of the ballast bed is to provide a bearing for rails, resistance to sleepers, to keep the geometry of track, and responsible for draining water away from the track and elastics of the tracks. With the development of railway, the axle load and the speed of trains increase largely, putting a higher requirement for the function of ballast track bed [1]. To keep the safety and stability of railway, more and more frequent maintenance is needed, such as tamping and ballast renewal. As a consequence, the consumption of materials and labours, during those maintenance processes, causes great economic costs and environmental problems. Prolong the life span of ballast track by reinforcement method and sustainable railway systems using recycled materials are needed to be studied.

In one aspect, several methods are used to reinforce ballast layer, for example, the use of geogrid increase the resistance between ballast and decrease the settlement [2], and it can be used not only in ballast layer but also in sub-ballast [3,4], geocell has the similar function with geogrid in reinforcement [5]. Elastic mat or pad (ballast mat, rail pad, and under sleeper pad) can increase the elastic, decrease the vibration, and enlarge the area of force distribution thus decrease the process of ballast degradation [6–8].

* Corresponding author.
E-mail address: gqjing@bjtu.edu.cn (G. Jing).

https://doi.org/10.1016/j.conbuildmat.2021.123114
0950-0618/

Polyurethane can bond ballast in the contact point thus increase the capacity and keep the drainage ability at the same time [9,10]. Those reinforcement methods all show their effect and have been proved in practice.

In another aspect, using recycled materials is also a good way for sustainable development. For example, the rubber from tires can be a resource for rubber mat or pad manufacture [11], directly added crushed rubber into ballast layer also can decrease the ballast degradation [12–14]. Research on the degraded ballast shows that it can be reused by mixed with fresh ballast [15]. Another material is slag, which is a byproduct of iron production (around 12%–16% slag by weight is generated [16]). Based on this huge amount and the similar properties with crushed stone, slag has used in construction, also drew the attention of railway area.

Slag can be divided into furnace slag and steel slag, according to the different process in iron steel making. Furnace slag is a byproduct in the first stage when using iron ore to produce pig iron, and steel slag is a byproduct when using the iron to produce steel. Among them, steel slag can replace granular materials in normal concrete manufacture [17–19], asphalt concrete [20] and pavement [21]. With a similar property of stone, and even better prosperities in interlock performance, higher density (3100–3500 kg/m^3), and high resistance to abrasion [22,23], steel slag also can be used in the ballast layer. Delgado et al. [16] studied the mechanical performance of inert steel slag ballast by comparing it with granite ballast (both of them are scaled with 1:2.5 size), results show that slag has higher shear strength and lower deformation in long-term behaviour. Esmaeili et al. [22] did the comparing tests on lateral resistance between steel slag and limestone ballast, results show a 27% increase can be observed by using steel slag. Morata et al. [24] employed steel slag as track bed layer, and results show it has an improvement in track stiffness, track stability, bearing capacity (strength), and durability. Although those research shows the good performance of steel slag in railway system, a vital problem of electrical conductivity exists, because of the chemical composition of steel slag [25]. This property will cause communication problems for railway safety.

Another kind is furnace slag with a particle size of 10–30 mm. It has a smaller density than steel slag, the value is around 2000 kg/m^3, the strength is also lower than steel slag. With those properties, furnace slag is considered not a proper material for the ballast layer. But in another way, it can be a resource for sub-ballast.

Sub-ballast is a granular layer provided bearing to ballast layer, and as a filter to provided ballast directly contact with soil foundation or soil fill in ballast layer under cyclic loading [26,27]. The requirement of physical properties for sub-ballast is a lot lower than ballast, i.e. the Los Angeles Abrasion index (LAA), compression strength, the Particle size distribution is in a range from 0.075 mm to 45 mm, and it has no electrical conductivity requirement. Indraratna et al. [28] studied several parameters (the permeability, stress-strain behaviour, strain energy absorption, particle breakage, swell pressure, and axial displacement under cyclic loading) of the mixture of furnace slag, coal wash, and rubber crumbs working as sub-ballast. The results of Indraratna et al. [28] show that by controlling the ratio of different materials, the mixture can reach higher performance than the traditional sub-ballast.

Based on the researches mentioned above, it is possible to use furnace slag as sub-ballast. Thus, aiming to find out the behaviour of furnace slag for sub-ballast, this study conducted a series of tests and simulations, and a comparison between crushed stone was analysed. The direct shear tests were employed to show the shear performance, Single Particle Crushing Tests (SPCT) and LAA tests were employed to show the strength and the resistance to abrasion, the image analysis based on 3D scanning is used to show the shape property, and simulations based on DEM was used to show the shear behaviour in mesoscopic.

2. Material specification

Furnace slag used in this research is shown in Fig. 1(a), its density is 2250 kg/m^3. With the function of filter, the particle size of sub-ballast needs to stay in a range of Particle Size Distribution (PSD), which is shown in Fig. 2. So, the slag was sieved and remixed, and the PSD curve is also shown in Fig. 2. In comparison, the traditional sub-ballast is granite material, i.e. the crushed stone, and it is showed in Fig. 1(b), with the density of 2800 kg/m^3, and it is saved and mixed by the same PSD with furnace slag.

2.1. Single particle crushing strength

During the daily operation of railway, particle breakage is a key process contributing to degradation, thus SPCT was employed to find out the crushing property of single particle, and the test device is shown in Fig. 3. During this test, the sample was crushed by stress controlling method, i.e. after located the slag, the loading plate was moving with a certain force to time speed (0.1 kN/s) until the particle breakage happened. The stress-displacement curve was supervised by the auto-controlling system. During the crushing process, the breakage is initiated with the fracture by tensile failure, and it can be described with Eq. (1) [29]. Due to the influence of particle size, 3 different size (5 mm 10 mm and 20 mm) was selected, and each size included 5 particles.

$$\sigma = F/d^2 \tag{1}$$

where d is the diameter of particle which is also related to the distance of loading plate and the platform, F is the compressive force, andσ is the tensile stress.

The peak compressive force, sorted different particle sizes, is shown in Fig. 4(a), and the tensile strength, calculated refer to Eq. (1), is shown in Fig. 4(b). Because the crushing test is not only related to particle size, but also the loading point, loading direction, and particle geometry. The peak compressive force and the tensile strength are shown with a range where 5 particles for each size are included. Especially for furnace slag, the inner void is in an inhomogeneous distribution, thus the test results show a relatively wide range. In Fig. 4, it is obvious that the strength of furnace slag is higher than the traditional sub-ballast, the value increases 39%, 20%, 26% for 5 mm, 10 mm, and 20 mm, respectively. For both furnace slag and crushed stone, when the particle size increase, the peak compressive force is increased, but the tensile strength is decreased, thus proved that the bigger particle is more likely to break.

The crushing process can be explained by the displacement and force curve. In Fig. 5, the curve of 6 particles were drawn as representative, whose peak compressive force is approximate to the mean value. According to the curve, the crushing process began when the compressive force appears. The first stage is the initial contact of the loading plate and particle, it shows a slow increase of the compressive force, and some fluctuations were observed because of the angularity breakage. Those fluctuations are more obvious in the test for furnace slag due to the inner void. Then the second stage shows a linear relationship between the deformation and the force. After the compressive force reaches a peak value, the curve shows a linear decrease, indicating the final failure.

Except for 5 mm particles, for which the existence of fluctuation affects the analysis, the second stage of the crushing can be regarded as an elastic shortening process, and it presents the stiffness of the material. By calculating the slope, the stiffness of 10 mm furnace slag is 1.78e6N/m–3.75e6N/m, 20 mm furnace slag is 2.14e6N/m–2.52e6N/m, and the value for 10 crushed stone is 2.11e6N/m–3.93e6N/m, 20 mm crushed stone is 1.42e6N/m–2.25

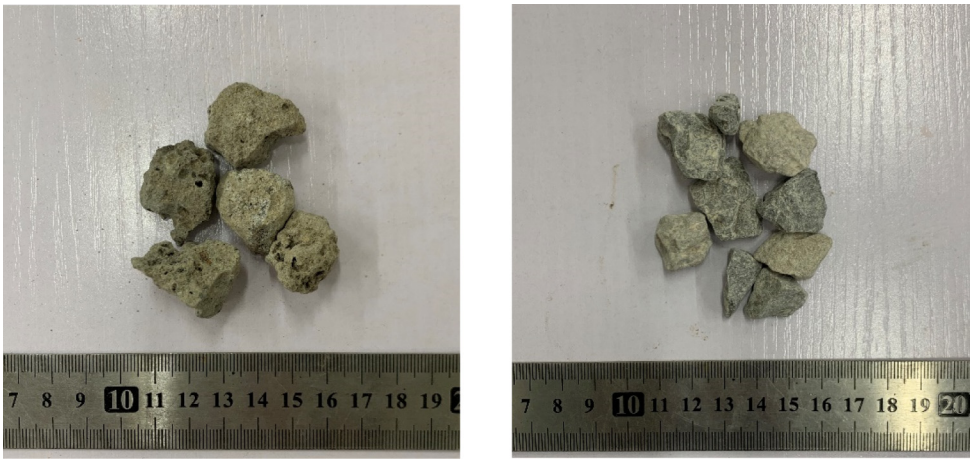

(a) Furnace slag (b) Crushed stone

Fig. 1. Material for tests.

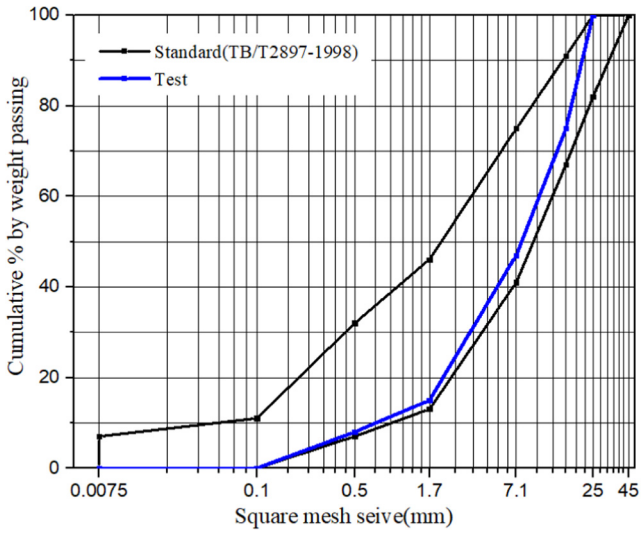

Fig. 2. Particle size distribution for sub-ballast.

N/m, as shown in Table 1. However, results are in a relatively big range, it can be seen that furnace slag has a higher stiffness than crushed stone.

2.2. Resistance to abrasion

In addition, the abrasion resistance is shown by LAA tests, as shown in Fig. 6. For sub-ballast, the test sample should be departed into 2 parts: 10–16 mm particle 2500 g, and 16–20 mm particle 2500 g. 8 iron balls, with a total weight of 3330 ± 20 g, are mixed in the chamber. The test is conducted with the chamber rotates 500 rounds (31–33 r/min) [30], During this process, the particle is facing impaction and abrasion, and after the tests, the aggregate should be re-sieved and cleaned and weighted, and calculated by Eq. (2).

$$LAA = \frac{G_1 - G_2}{G_1} \times 100\% \quad (2)$$

The Los Angeles abrasion index (LAA, %) is defined by Eq. (2), where G_1 is the total weight of particle before abrasion (g), and G_2 is the weight of particle size bigger than 1.7 mm after abrasion (g). The test value for furnace slag is 26.04%, and crushed stone is 31.28%. However, in the SPCT, furnace slag showed angularity breakage in the initial stage which may increase the LAA, the

(a) Test device (b) Crushing plate

Fig. 3. Single particle crushing test.

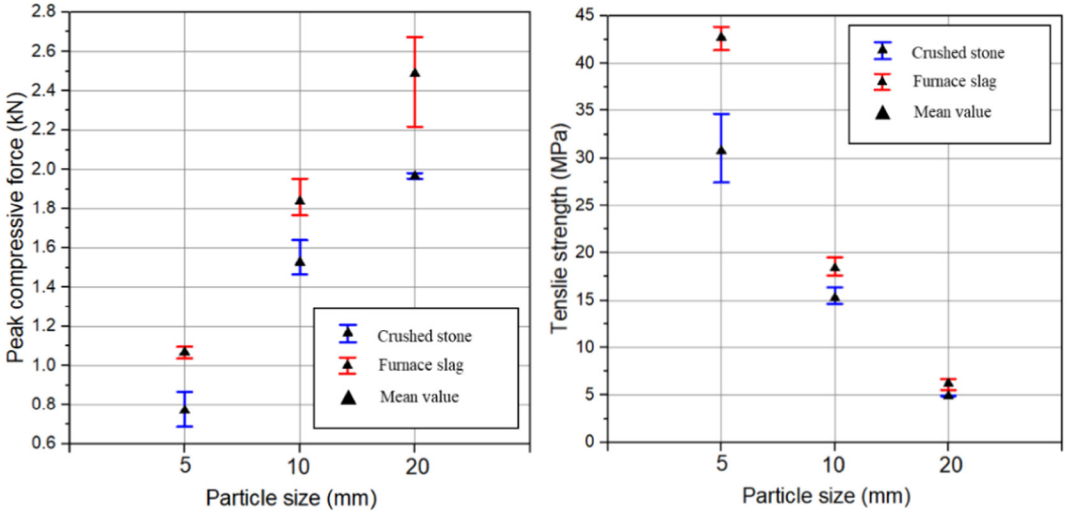

(a) Compressive force (b) Tensile strength

Fig. 4. Data of SPCT.

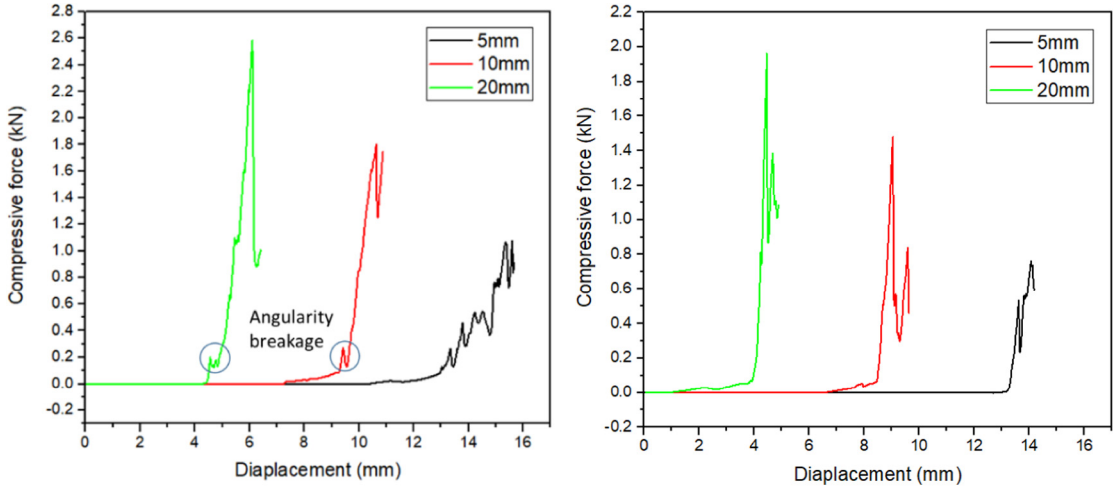

(a) Furnace slag (b) Crushed stone

Fig. 5. Displacement-compressive force curve.

Table 1
Particle stiffness according to SPCT (*e6N/m).

Material	Size	Particle 1	Particle 2	Particle 3	Particle 4	Particle 5	Average
Furnace slag	10 mm	3.48	2.56	3.18	3.75	1.78	2.95
	20 mm	2.00	2.52	2.11	2.14	2.42	2.23
Crushed stone	10 mm	3.24	2.29	2.11	3.93	2.77	2.87
	20 mm	2.19	1.42	2.25	1.55	2.01	1.88

abrasion resistance is higher than the traditional sub-ballast. Overall, the SPCT and LAA show that furnace slag has better performance both on the resistance to breakage and abrasion.

3. Experimental tests

3.1. Direct shear test

The direct shear test apparatus is shown in Fig. 7. Size scale in a direct shear test is an important factor, which will influence the accuracy of the result, Jewell et al. [31] suggested that the length of the shear box compare with the D_{50} should be larger than 50, Wang et al. [32] suggest that the size of the shear box should be at least 60 times larger than particle size for sand, and the standard ASTM D 3080-90 [33] suggested that the values should be larger than 10. In this research, the apparatus consists of a lower box and an upper box, with both size of 300 mm * 300 mm * 100 mm. The D_{50} of the sample with the PSD (as Fig. 2) is around 7.1 mm, and the biggest particle size is around 25 mm. The sample is loaded and compacted in the shear box, and a plate which covering the

(a) Test apparatus (b) Sample with iron ball inside the chamber

Fig. 6. Los Angeles abrasion.

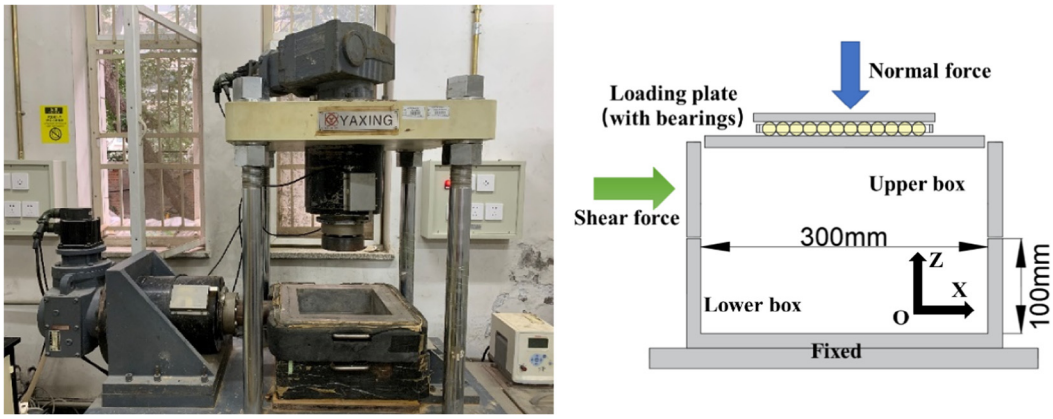

(a) Test apparatus (b) Schematic diagram

Fig. 7. Direct shear test apparatus.

sample is used to transmit the normal pressure. A bearing set is put on the plate to keep the loading and diminish the friction between the upper box and the servo loading jack. Then the servo system begins to work which controls the normal stress of 50 kPa 100 kPa and 200 kPa corresponding to different test conditions. During the shear process, the upper box is moving with a speed of 0.2 mm/min until the shear strain reaches 10% (30 mm shear displacement), the shear stress, strain, and dilatancy are automatically recorded by the computer.

Test results are shown in Fig. 8. It should be noticed that, for furnace slag under 200 kPa normal pressure, there is a drop-down occurred around 22 mm displacement, due to some slide happened in the box. And, an increase with fluctuation can be seen in the end state. However, those trends are different from others,

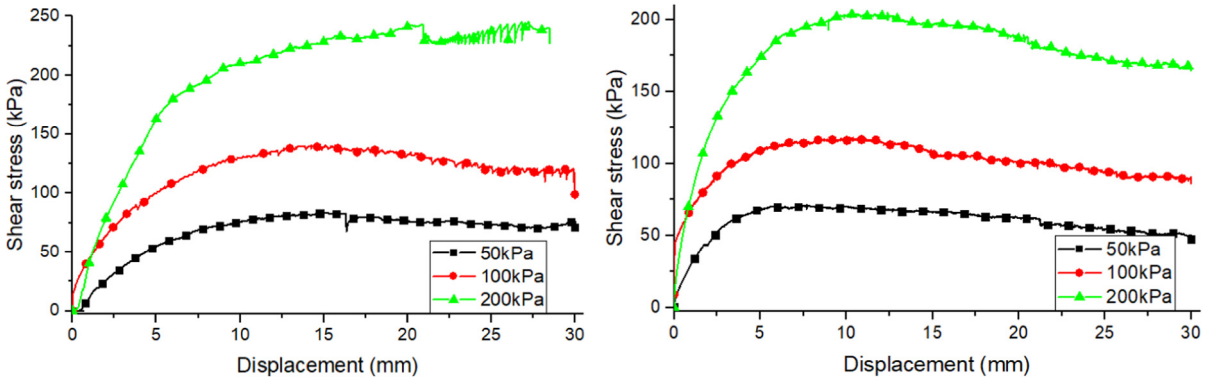

(a) Furnace slag (b) Crushed stone

Fig. 8. Displacement-shear stress curve.

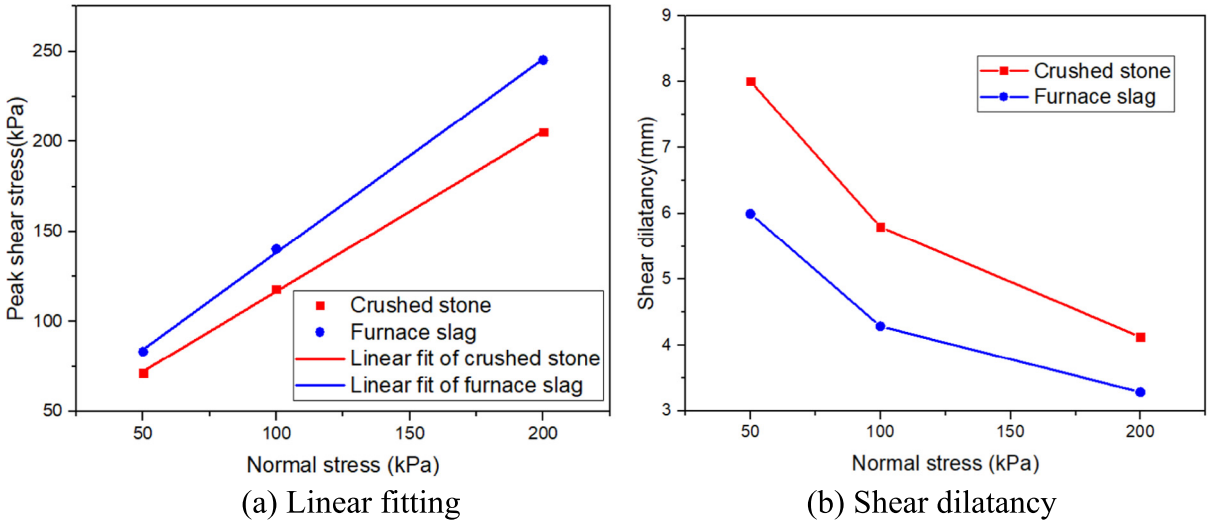

Fig. 9. Peak shear stress and shear dilatancy.

the result is still valid because the peak force is observable. The peak shear stress of furnace slag is 83.27 kPa, 140.25 kPa, 245.28 kPa, and for crushed stone, the peak shear stress is 71.50 kPa, 117.95 kPa, 205.29 kPa, both of them are according to normal stress 50 kPa, 100 kPa, 200 kPa, respectively. It can be seen that furnace slag all shows an increase than the traditional sub-ballast under 3 different normal stress. The increase reaches 16.46%, 18.91%, and 19.48%.

In addition, the normal stress and peak shear stress of different condition is shown in Fig. 9(a). The linear fitting is related to 2 constants, the cohesion and the tangent of friction angle. The use of furnace slag increases the frictional angle from 41.65 to 47.09°, comparing with crushed stone. The cohesion of furnace slag presents a bigger value than crushed stone, which is 30.75 kPa and 27.83 kPa, respectively. Since the same PSD is used for those 2 materials, the increase in friction angle and cohesion is mainly related to the particle shape and surface texture. In Fig. 9(b), the final shear dilatancy of furnace slag is 5.99 mm, 4.28 mm, 3.28 mm, corresponding to the normal stress 50 kPa, 100 kPa, and 200 kPa, and the value for crushed stone is 8.01 mm, 5.80 mm, and 4.12 mm, respectively. The 20.44%–26.04% decrease in dilatancy also indicates that furnace slag has better shear performance than crushed stone.

3.2. Stiffness tests

The stiffness tests were carried by the same device with direct shear tests (Fig. 7), only changing the loading part with a 150 mm diameter disk. The loading process for this part was realised by controlling the loading disk downward at a certain speed (0.2 mm/min) which can be regarded as a quasi-static loading process, and the stop condition is when the displacement reaches 4 mm. During the test, displacement and force are recorded for stiffness calculation.

Test results are shown in Fig. 10. For furnace slag, the peak compressive force is 14.41 kN, (815.57 kPa), and the displacement at peak force is 3.15 mm. For crushed stone, the peak compressive force is 11.89 kN, (673.02 MPa), and the displacement at peak force is 2.06 mm. Under this test condition, the stiffness of furnace slag is 4.57e6 N/m, and the value for crushed stone is 5.77e6 N/m. Thus, the capacity and elasticity of furnace slag are all better than crushed stone. In addition, the numerical simulation for this test

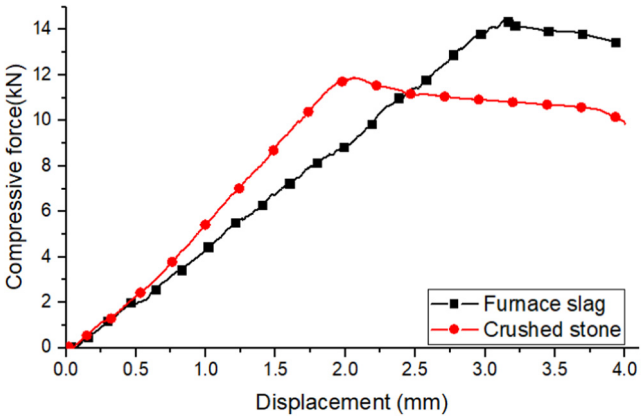

Fig. 10. Test results for box stiffness.

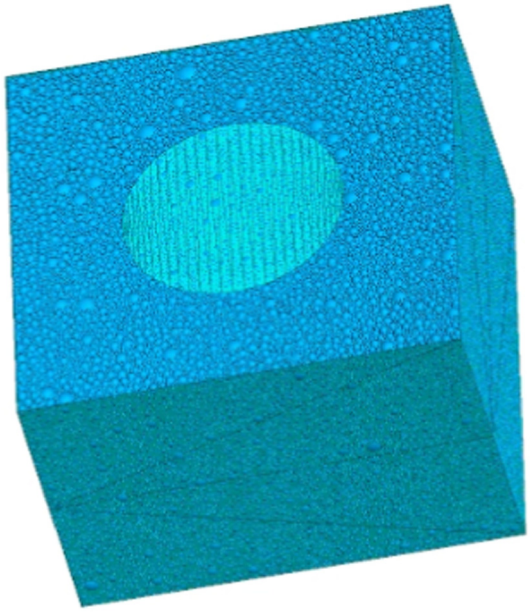

Fig. 11. Model after initial balance.

Table 2
Parameters of linear contact model in simulations.

Parameters	Furnace slag	Crushed stone	Box
Tangential stiffness (N/m)	2.7e6	2.2e6	1e8
Normal stiffness (N/m)	2.6e6	2.3e6	1e8
Friction coefficient	0.5	0.4	0.2
Mass density (kg/m^3)	2250	2800	–
Damping coefficient	0.7	0.7	–

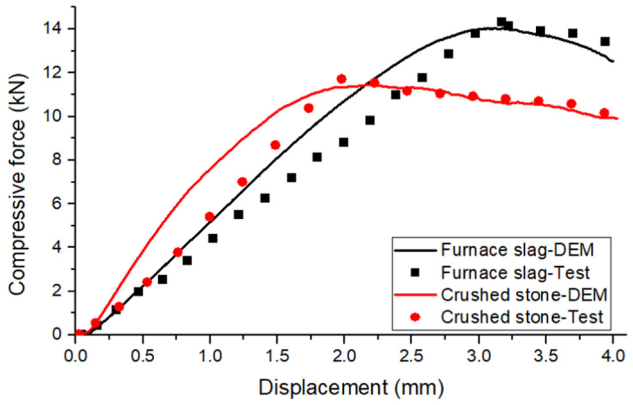

Fig. 12. Validation for DEM model.

was used to analyse the contact and force distribution in the following.

4. Numerical simulations

DEM is a method used to analysis the mesoscopic characteristic of aggregate materials, the coordination number, stress distribution, and contact force, and displacement can be shown by this method. In this study, the simulation of box stiffness test was carried out, and the simulation was conducted with the software PFC^{3D}. In accordance with the laboratory test, the model builds a 300 mm * 300 mm * 200 mm box and a 150 mm diameter loading plate, these two components are both "wall" element. This element can bear force but cannot transfer force, so the loading process was conducted by applying a Z-velocity, and the macroscopic result was recorded by supervising the displacement and counterforce of the plate. Due to the particle size and porosity, the model contains more than 500,000 particles. Considering the model scale, particle size and time consumption problem, the model uses "ball" element to present the aggregate material. The model is shown in Fig. 11 In addition, to differentiate furnace slag and crushed stone, the "kn" (shear stiffness) and "ks" (tangential stiffness) in a linear contact model were set referring to the average value of the results of SPCT. According to the direct shear test, the frictional furnace slag is higher than crushed stone, thus a higher frictional coefficient is set for furnace slag model. Together with the reference from previous researches [34–36], the final parameter is shown in Table 2, and the validation is provided by the deformation and force curve in Fig. 12, where the curve of simulation fitted the test results.

In Fig. 12, the peak force of furnace slag is 14.03 kN (14.41 kN in laboratory test), and the displacement at peak force is 3.11 mm (3.15 mm in laboratory test). For crushed stone, the peak compressive force is 11.44 kN (11.89 kN in laboratory test), and the displacement at peak force is 2.16 mm (2.06 mm in laboratory test).

Fig. 13 shows the force chain at the peak state and finish state of the simulation, where the line presents the contact and the colour presents the value of the force. In Fig. 13(a) and (c), the peak state shows a denser force chain than the finish state in Fig. 13(b) and (d). Especially in the top corner, along with the loading process after peak state, ballast in this area gradually loses its function. It is because under the unconfined top layer (except the loading plate), the interlock between ballast is broken. When compared the two materials, it's obvious that furnace slag shows a denser force chain and wider distribution, as the dash line, it provides the explanation for the macroscopic result. In detail, at the peak

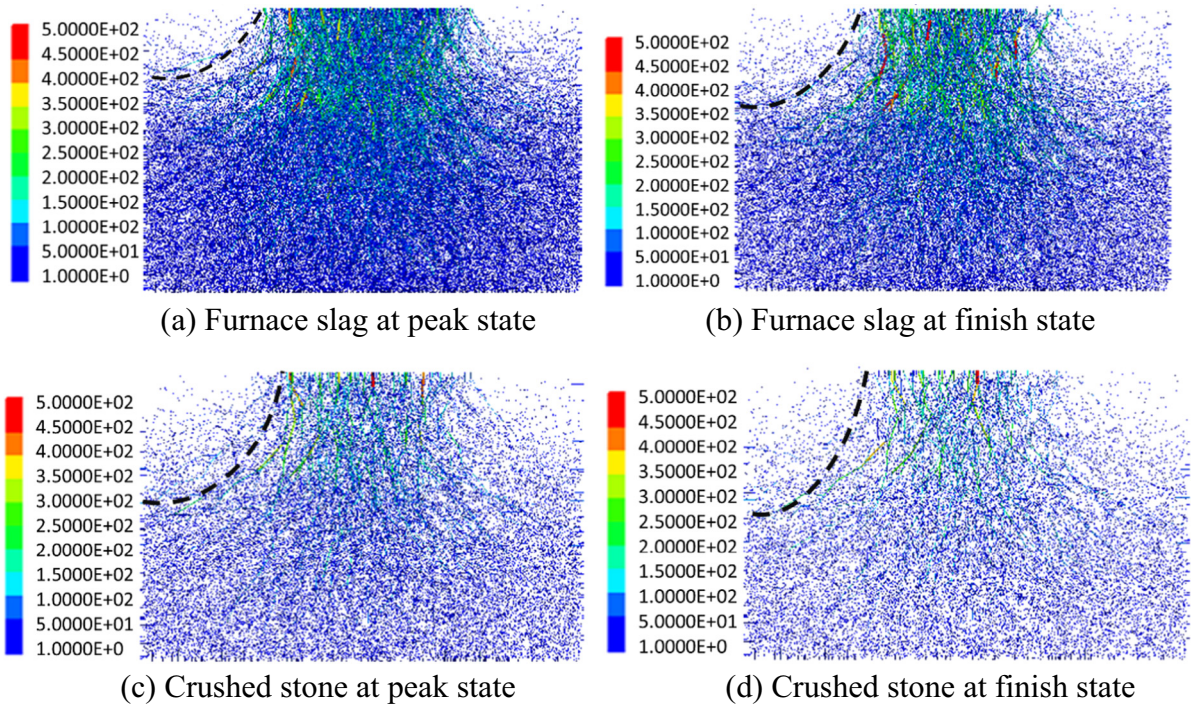

Fig. 13. Force chain (unit: N).

state, the maximum contact force is 0.57 kN and 0.46 kN, at the finish state, the value is 0.75 kN and 0.67 kN, for furnace slag and crushed stone respectively. From peak state to finish state, the maximum contact force is increased, this behaviour is related to the force chain changes. During this process, force in some contacts exceeds the maximum capacity, thus leading to failure. With those contact no longer contributing, and the loading continuing, the force in left effective contacts increase. Because the increase only happened in some contacts between the particle and the loading plate, as shown in Fig. 13(b) and (d), it cannot offset the overall decrease trend of compressive force.

5. Conclusion

This research introduces the use of furnace slag as sub-ballast in railway construction. Furnace slag is a byproduct of using iron ore to produce pig iron, because of its characteristic, the reuse of furnace slag is not as wide as steel slag. However, compared with the requirement of the railway sub-ballast, furnace slag can be a good material, also works for environmental-friendly development. Several experimental tests were employed, including the Single Particle Crushing Test (SPCT), the Los Angeles abrasion Test (LAA), the direct shear test, and the box stiffness tests, and the crushed stone (i.e. the traditional material for sub-ballast) was tested as the comparison. In addition, a DEM simulation in accordance with the box stiffness test was carried. The main conclusions are listed below:

1. In SPCT, furnace slag shows a 20%–39% increase in peak compressive force than the crushed stone. The result indicated that furnace slag is better in the resistance of particle breakage.
2. However, furnace slag shows more angularity breakage, the LAA value is still lower than crushed stone. It indicated a better resistance to abrasion, where the value for furnace slag is 26.04%, and for crushed stone is 31.28%.
3. In direct shear tests, furnace slag shows 16.46%, 18.91%, and 19.48% increase than crushed stone, corresponding to normal stress 50 kPa, 100 kPa, and 200 kPa respectively. Also, the performance of furnace slag is better in frictional angle, cohesion, and shear dilatancy.
4. In the box stiffness, the peak compressive force of furnace slag is 14.41 kN, (815.57 kPa). For crushed stone, it is 11.89 kN, (673.02 MPa). Under this test condition, the stiffness of furnace slag is 4.57e6N/m, and the value for crushed stone is 5.77e6N/m.
5. In the DEM model for box stiffness was built, furnace slag shows better performance than crushed stone in contact and force distribution.

Declaration of Competing Interest

The authors declare that they have no known competing financial interests or personal relationships that could have appeared to influence the work reported in this paper.

References

[1] C. Esveld, Modern Railway Track, MRT-Productions, The Netherlands, 2001.
[2] Buddhima Indraratna, Sanjay Nimbalkar, Tim Neville, Performance assessment of reinforced ballasted rail track, Proc. ICE: Ground Improvement 167 (1) (2014) 24–34.
[3] X. Chen, Y. Jia, J. Zhang, Geogrid-reinforcement and the critical state of graded aggregates used in heavy-haul railway transition subgrade, Transp. Geotech. 11 (2017) 27–40.
[4] M.M. Biabani, B. Indraratna, S. Nimbalkar, Assessment of interface shear behaviour of sub-ballast with geosynthetics by large-scale direct shear test, Proc. Eng. 143 (2016) 1007–1015.
[5] B. Indraratna, M.M. Biabani, S. Nimbalkar, Behavior of geocell-reinforced subballast subjected to cyclic loading in plane-strain condition, J. Geotech. Geoenviron. Eng. 141 (1) (2015).
[6] L. Le Pen et al., Behaviour of under sleeper pads at switches and crossings – field measurements, Proc. Inst. Mech. Eng. F: J. Rail. Rapid Transit. 232 (4) (2018) 1049–1063.
[7] S. Kaewunruen, A.M. Remennikov, Sensitivity analysis of free vibration characteristics of an in situ railway concrete sleeper to variations of rail pad parameters, J. Sound Vib. 298 (1–2) (2006) 453–461.
[8] M. Sol-Sánchez, F. Moreno-Navarro, M.C. Rubio-Gámez, The use of elastic elements in railway tracks: a state of the art review, Constr. Build. Mater. 75 (2015) 293–305.
[9] G. Jing et al., Polyurethane reinforced ballasted track: review, innovation and challenge, Constr. Build. Mater. 208 (2019) 734–748.
[10] P.K. Woodward et al., Study of railway track stiffness modification by polyurethane reinforcement of the ballast, Transp. Geotech. 1 (4) (2014) 214–224.
[11] M. Sol-Sánchez, F. Moreno-Navarro, M.C. Rubio-Gámez, An analysis of the performance of deconstructed tires for use as pads in railroad tracks, J. Civ. Eng. Manage. 22 (6) (2016) 739–746.
[12] Y. Guo et al., Effects of crumb rubber size and percentage on degradation reduction of railway ballast, Constr. Build. Mater. 212 (2019) 210–224.
[13] M. Sol-Sánchez et al., An alternative sustainable railway maintenance technique based on the use of rubber particles, J. Cleaner Prod. 142 (2017) 3850–3858.
[14] B. Indraratna et al., Performance of rubber tire-confined capping layer under cyclic loading for railroad conditions, J. Mater. Civ. Eng. 30 (3) (2018).
[15] W. Jia et al., Experimental and numerical investigations on the shear behaviour of recycled railway ballast, Constr. Build. Mater. 217 (2019) 310–320.
[16] B.G. Delgado et al., Mechanical behavior of inert steel slag ballast for heavy haul rail track: laboratory evaluation, Transp. Geotech. 20 (2019).
[17] M. Oge et al., An overview of utilization of blast furnace and steelmaking slag in various applications, Mater. Today: Proc. 11 (2019) 516–525.
[18] J. Huang et al., Effect of recycled fine aggregates on alkali-activated slag concrete properties, Structures 30 (2021) 89–99.
[19] M.A. Ridho et al., Recycled aggregates concrete compressive strength prediction using artificial neural networks (ANNs), Infrastructures 6 (2) (2021).
[20] Q. Li et al., Evaluation of basic oxygen furnace (BOF) material into slag-based asphalt concrete to be used in railway substructure, Constr. Build. Mater. 115 (2016) 593–601.
[21] J.J. Emery, Slag Utilization in Pavement Construction, Extending Aggregate Resources, ASTM STP 774, American Society for Testing and Materials, 1982, pp. 95–118.
[22] M. Esmaeili, R. Nouri, K. Yousefian, Experimental comparison of the lateral resistance of tracks with steel slag ballast and limestone ballast materials, Proc. Inst. Mech. Eng. Part F: J. Rail Rapid Transit. 231 (2) (2017) 175–184.
[23] L.V. Fisher, A.R. Barron, The recycling and reuse of steelmaking slags – a review, Resour. Conserv. Recycl. 146 (2019) 244–255.
[24] M. Morata, C. Saborido, V. Fontserè, Slag aggregates for railway track bed layers: monitoring and maintenance, in: Computers in Railways XV Railway Engineering Design and Operation, 2016, pp. 283–294.
[25] C. Shi, Steel slag – its production, processing, characteristics, and cementitious properties, J. Mater. Civ. Eng. 16 (3) (2004) 230–236.
[26] L. Dominic, B. Indraratna, Assessment of subballast filtration under cyclic loading, J. Geotech. Geoenviron. Eng. 136 (11) (2009) 1519–1528.
[27] A.S.J. Suiker, E.T. Selig, R. Frenkel, Static and cyclic triaxial testing of ballast and subballast, J. Geotech. Geoenviron. Eng. 131 (771–782) (2005).
[28] B. Indraratna, Y. Qi, A. Heitor, Evaluating the properties of mixtures of steel furnace slag, coal wash, and rubber crumbs used as subballast, J. Mater. Civ. Eng. 30 (1) (2018).
[29] J.C. Jaeger, Failure of rocks under tensile conditions, Int. J. Rock Mech. Mining Sci. Geomech. Abstracts 4 (2) (1967) 219–227.
[30] TB/T2328.1-18 Test Method for Railway Ballast, Ministry of Railway, China, 1992.
[31] R.A. Jewell, C.P. Worth, Direct shear tests on reinforced sand, Geotechnique 37 (1) (1987) 53–68.
[32] J. Wang, M. Gutierrez, Discrete element simulations of direct shear specimen scale effects, Géotechnique 60 (5) (2010) 395–409.
[33] D. ASTM, Standard Test Method for Direct Shear Tests of Soils Under Consolidated Drained Conditions, ASTM, West Conshohocken, 1990.
[34] F. Khatibi, M. Esmaeili, S. Mohammadzadeh, DEM analysis of railway track lateral resistance, Soils Found. 57 (4) (2017) 587–602.
[35] E. Tutumluer et al., Discrete element modelling of ballasted track deformation behaviour, Int. J. Rail Transp. 1 (1–2) (2013) 57–73.
[36] X. Bian et al., Micromechanical particle interactions in railway ballast through DEM simulations of direct shear tests, Int. J. Geomech. 19 (5) (2019).